Available online at www.sciencedirect.com
SCIENCE DIRECT®
ELSEVIER
Nuclear Instruments and Methods in Physics Research B 235 (2005) 535–539
NIM B Beam Interactions with Materials & Atoms
www.elsevier.com/locate/nimb

Optimization of the energy resolution of an ideal ESCA-type hemispherical analyzer

T.J.M. Zouros [a,b,*], E.P. Benis [c,1], I. Chatzakis [c]

[a] Department of Physics, University of Crete, P.O. Box 2208, 71003 Heraklion, Crete, Greece
[b] Institute of Electronic Structure and Laser, P.O. Box 1527, 71110 Heraklion, Crete, Greece
[c] James R. Macdonald Laboratory, Department of Physics, Kansas State University, Manhattan, KS 66506-2604, USA

Available online 29 April 2005

Abstract

The overall base resolution $\Re_B$ of a high throughput ideal hemispherical deflector analyzer (HDA) equipped with a zoom lens and a position sensitive detector (PSD) placed a distance h from the exit focus plane of the HDA is investigated as a function of h, pre-retardation factor F and beam angle θ_0. $\Re_B$ is in general a function of the linear lens magnification $|M_L|$ and can be minimized by choosing the optimal linear lens magnification $|M_L|_o$ under the constraints of the Helmholtz–Lagrange law. Thus, the optimal resolution, $\Re_B(|M_L|_o)$ can be computed as an analytic function of h, F, θ_0 and represents the ultimate resolution that can be attained ignoring fringing field effects. These results should be helpful in the efficient design and performance evaluation of any HDA utilizing a focusing lens and PSD as is typical for ESCA-type electron spectrometers.

PACS: 07.81.+a

Keywords: Hemispherical deflector analyzer; Energy resolution; Electron spectroscopy

1. Introduction

High resolution electron spectroscopy, e.g. electron spectroscopy for chemical analysis (ESCA), is a mature technique utilized in many different fields of physics, material science, chemistry and even biology and medicine. One of the most popular spectrometers in use today is the hemispherical deflector analyzer (HDA). Today's, modern high power HDAs are equipped with state-of-the art

* Corresponding author. Address: Department of Physics, University of Crete, P.O. Box 2208, 71003 Heraklion, Crete, Greece. Tel.: +30 2810 394117; fax: +30 2810 394101.

E-mail address: tzouros@physics.uoc.gr (T.J.M. Zouros).

[1] Present address: Institute of Electronic Structure and Laser, P.O. Box 1527, 71110 Heraklion, Crete, Greece.

0168-583X/$ - see front matter © 2005 Elsevier B.V. All rights reserved.
doi:10.1016/j.nimb.2005.03.239

multi-element zoom lens and position sensitive detector (PSD) [1–5] and therefore enjoy a very large collection efficiency. The zoom lens focuses the source electrons onto the HDA entry, thus increasing the overall collection solid angle. Pre-retardation, also supplied by the lens, may be used to further improve the overall energy resolution of the entire spectrometer by decelerating the particles from an initial source energy T down to a much lower energy t just prior to HDA entry.

For an ideal HDA, the exit radius r_π (after deflection by 180° inside the HDA) is given in terms of the entry radius r_0 and incident angle $\alpha^\star$ by [6]:

$$r_\pi \equiv r_\pi(r_0, \alpha^\star, \tau) = -r_0 + \frac{D_0}{1 + \kappa(1 - \tau\cos^2\alpha^\star)}, \quad (1)$$

with

$$\tau \equiv t/w, \quad (2)$$

$$\kappa \equiv \xi/\gamma, \quad (3)$$

$$\xi \equiv R_\pi/R_0 \geqslant 1, \quad (4)$$

$$\gamma \equiv 1 - V(R_0)/w \geqslant 1, \quad (5)$$

$$D_0 \equiv R_0 + R_\pi = (1 + \xi)R_0 \geqslant 2R_0, \quad (6)$$

$$V(r) = -k/r + c, \quad (7)$$

$$qk = wD_0/\kappa, \quad (8)$$

$$qc = w(1 + \kappa). \quad (9)$$

The HDA is tuned to the central ray energy w [7] and the voltages are set once w and γ are specified. The parameter γ controls the potential at the entry position of the central ray, $V(R_0)$, where in general $V(r)$ is the assumed *ideal* $1/r$ potential inside the HDA, with constants k and c defined via the central trajectory [6] and given above for a particle of charge q (for electrons $q = -|e|$ with $e = 1.61 \times 10^{-19}$ C). A conventional HDA is usually non-biased, since $V(R_0)$ is matched to the energy of the central ray w so that $\gamma = 1$. For a *biased* HDA we always have $\gamma > 1$ [6]. D_0 is the characteristic range of the central ray which enters with $\alpha^\star = 0$ at $r = R_0$ and exits at $r = R_\pi$. For a conventional HDA, the central ray describes a circle so that $R_0 = R_\pi = \overline{R}$ (where $\overline{R} = \frac{1}{2}(R_1 + R_2)$ with R_1 and R_2 the inner and outer radii of the HDA) and therefore $\xi = 1$. For a paracentric HDA $R_0 < R_\pi$ and therefore $\xi > 1$ and the orbit is an ellipse. The general ray will have a nominal pass energy t and therefore $\tau = t/w$ is the "reduced" or fractional pass energy. Thus, the central ray will have $\tau = 1$. The parameter κ characterizes the degree of paracentricity and biasing of the HDA [6]. Eq. (1) describes both conventional and paracentric HDAs. For the conventional HDA we just set $\kappa = \gamma = \xi = 1$ and $D_0 = 2\overline{R}$.

The ideal biased paracentric HDA is found to focus to first order in the angle $\alpha^\star$ after deflection of 180°. Thus, ideally, a PSD should be placed so that it lies along the focus plane at $h = 0$ (see Fig. 1). However, due to practical geometry constraints, typically $h > 0$. Here we include h in our analysis and investigate its effect on the base resolution. On exiting the HDA, the charged particle is again refracted at the potential boundary and then travels through the drift region, impinging on the PSD plane at the axial distance $r_{\pi h}$, as shown in Fig. 1, given by:

$$r_{\pi h} = r_\pi + h\tan\alpha_\pi^\star, \quad (10)$$

where $\alpha_\pi^\star$ is the divergence angle on the exit side of the HDA focusing plane (after refraction). Using the relation between $\alpha_\pi^\star$ and $\alpha^\star$ [6], we can then write:

$$r_{\pi h} \equiv r_{\pi h}(r_0, \alpha^\star, \tau, h) = r_\pi\left(1 - \frac{h}{r_0}\tan\alpha^\star\right). \quad (11)$$

Particle trajectories of nominal (reduced) pass energy τ_0, entering the HDA at radial distance r_0 and incidence angle $\alpha^\star$ within the ranges:

$$R_0 - \Delta r_0/2 \leqslant r_0 \leqslant R_0 + \Delta r_0/2, \quad (12)$$

$$-\alpha_\mathrm{m}^\star \leqslant \alpha^\star \leqslant \alpha_\mathrm{m}^\star \quad (13)$$

will in general give rise to a range $\Delta r_{\pi h}$ of exiting radii $r_{\pi h}$ values along the PSD that can be determined directly from Eq. (11). Here $\alpha_\mathrm{m}^\star > 0$ is the maximum possible angle allowed by the lens and analyzer geometry and settings, while Δr_0 is the size of the electron source (target) as imaged on the HDA entry by the lens and can therefore be directly controlled by the lens.

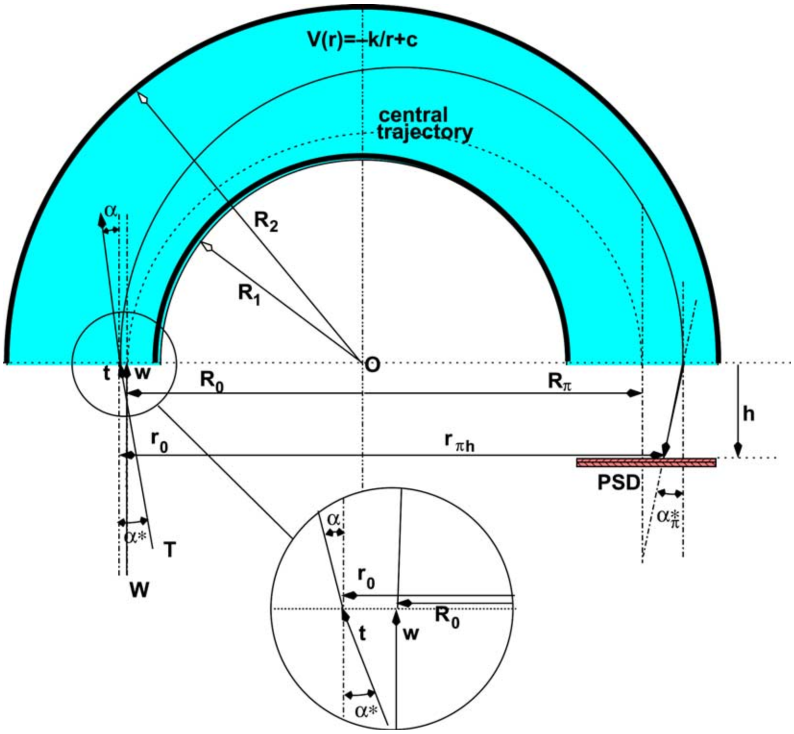

Fig. 1. Schematic geometry of an HDA. The central ray enters at R_0 with nominal energy w and $\alpha^\star = 0$, follows an elliptical trajectory and exits after deflection by 180° at R_π. Also shown is the trajectory of a ray entering at r_0 with $\alpha^\star$ and energy t and exiting at r_π with angle $\alpha^\star_\pi$ at the focus plane. It is detected at $r_{\pi h}$ on the position sensitive detector (PSD) offset by h from the HDA exit focusing plane.

2. Overall base resolution

The maximum radial range along the PSD, $\Delta r_{\pi h \max}$, dictates the base energy width from which the base energy resolution can be computed analytically by a series expansion to first order in Δr_0 and to second order in $\alpha^\star$ [8]. Skipping a lot of the required algebraic manipulations, we find that the mean (i.e. at $\tau = 1$) overall base resolution $\overline{\Re_\mathrm{B}}$, which also incorporates pre-retardation, is given by the double valued function:

$$\overline{\Re_\mathrm{B}} = \begin{cases} \frac{\Delta r_0 + \Delta r_\pi}{F\overline{D}} + \frac{2h}{F\overline{D}}\alpha^\star_\mathrm{m}\xi \\ \quad \text{for } 0 < \alpha^\star_\mathrm{m} \leqslant \overline{\alpha^\star_{\mathrm{m}0}}, \\ \frac{\Delta r_0 + \Delta r_\pi}{F\overline{D}} + \frac{h}{F\overline{D}}\alpha^\star_\mathrm{m}\left[(1+\xi)\left(1 - \frac{\Delta r_0}{2R_0}\right) - 1\right] + \frac{\alpha^{\star 2}_\mathrm{m}}{F} \\ \quad \text{for } \alpha^\star_\mathrm{m} \geq \overline{\alpha^\star_{\mathrm{m}0}} \end{cases} \tag{14}$$

with

$$\overline{\alpha^\star_{\mathrm{m}0}} = \frac{h}{\overline{D}}\left[(1+\xi)\left(1 + \frac{\Delta r_0}{2R_0}\right) - 1\right], \tag{15}$$

where $\overline{D} = D_0\kappa$ is just the mean energy dispersion length of the HDA. For $\kappa = 1$ (conventional HDA) we therefore have $\overline{D} = D_0$. The exit slit width or PSD resolution is given by Δr_π.

The two different branches in $\overline{\Re_\mathrm{B}}$ result from the two different maximum values of the radial base width $\Delta r_{\pi h \max}$ that can be attained under each condition. We note that both cases yield the same results at the special value of $\alpha^\star_\mathrm{m} = \overline{\alpha^\star_{\mathrm{m}0}}$. It can be readily shown that the first (upper) branch will always give rise to a finer base resolution. However, for $h = 0$, only the lower branch applies leading to the well known result for $\overline{\Re_\mathrm{B}}$:

$$\overline{\Re_\mathrm{B}} = \frac{\Delta r_0 + \Delta r_\pi}{F\overline{D}} + \frac{\alpha^{\star 2}_\mathrm{m}}{F}. \tag{16}$$

Table 1
List of actual spectrometer parameters [6]

$\overline{D}$	151.1 mm	Mean effective HDA dispersion
d_S	2.5 mm	Source diameter
l	264 mm	Source to entry pupil distance
d_p	4 mm	Entry pupil diameter
Δr_π	∼0.2 mm	PSD resolution
d_0	6 mm	HDA entry aperture diameter
h	15 mm	PSD to HDA focus plane distance
$\Delta\alpha_S = \frac{d_p}{2l}$	7.576 mrads	Source pencil half angle
$\Delta\Omega_S = \pi\Delta\alpha_S^2$	1.8×10^{-4} sr	Solid angle
$P + Q$	413 mm	Source to image distance

Refer also to Fig. 2.

The values of $\alpha_m^\star$ and Δr_0 are determined by the Helmholtz–Lagrange law for the particular geometry at hand. For conjugate object–image pairs the Helmholtz–Lagrange law [9–11] states that:

$$|M_L| \cdot |M_\alpha| = \sqrt{F} \tag{17}$$

with

$$\Delta r_0 = |M_L| d_S, \tag{18}$$

$$\alpha_m^\star = \theta_0 + |M_\alpha| \Delta\alpha_S, \tag{19}$$

where M_L and M_α are the linear and angular magnifications of the lens, respectively. We note that in general the beam angle θ_0 can be either positive or negative. Clearly, a zero beam angle is advantageous as the maximum effective opening angle into the HDA, $\alpha_m^\star$, will be minimized [8] with the corresponding improvement in the base resolution. Since in general it is hard to know exactly what the real value of θ_0 is, here we set it to zero. The more general treatment for θ_0, h ≠ 0 is given in Ref. [13].

Using Eqs. (17)–(19) in Eq. (14) it is seen that $\overline{\Re}_B$ is a function of $|M_L|$, $\overline{\Re}_B(|M_L|)$ and can be shown to have a minimum at $|M_L| = |M_L|_o$. This minimum can be readily found by setting $\partial\overline{\Re}_B/\partial|M_L| = 0$ and solving for $|M_L| = |M_L|_o$. The minimum base resolution $\overline{\Re}_B(|M_L|_o)$ is then the ultimate resolution that can be attained with the spectrometer. In [12], we have already presented results for $\theta_0 = h = 0$, a particularly simple case, which yields compact analytic results. Here, we give new results for the more general case where $h>0$. Again, the formulas are analytic, but much more cumbersome involving large expressions and therefore not presented in the limited space given here, but in Ref. [13]. To minimize errors, the analytical capabilities of the software program Mathematica were used to obtain the necessary results.

In Table 1 we give the values used in our calculation which correspond to the parameters of our actual spectrometer (Fig. 2).

Experimental measurements of the base resolution (computed as 2×FWHM), from Auger elec-

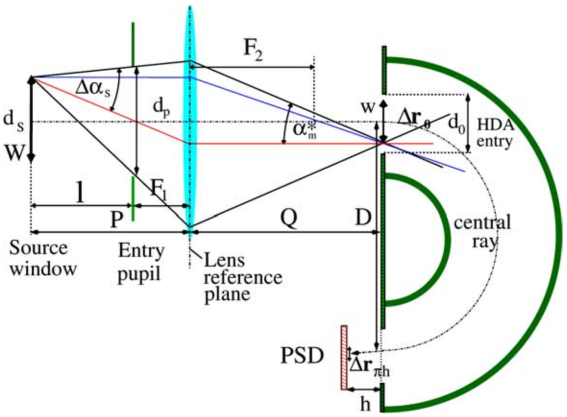

Fig. 2. Schematic geometry of a typical lens-HDA spectrometer. The source pencil (half-) angle, limited by the entry pupil, is imaged onto the HDA entry plane. The energy of the central ray, W at the source, is decelerated down to w just prior to HDA entry. When the HDA entry beam angle $\theta_0 = 0$ (not shown) [11], the Helmholtz–Lagrange law requires that for conjugate object–image pairs, $d_S\Delta\alpha_S\sqrt{W} = \Delta r_0\alpha_m^\star\sqrt{w}$. The drawing has been simplified by approximating the (thick) lens by a thin lens and is not to scale. The vertical dimensions are particularly enhanced in the case of the lens.

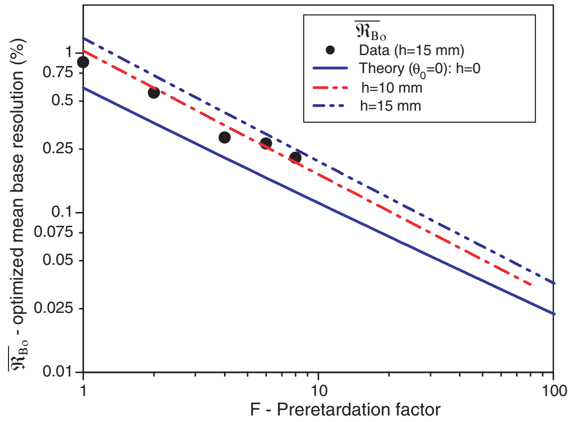

Fig. 3. Optimized mean base resolution $\overline{\Re_{Bo}}$ for beam angle $\theta_0 = 0$ plotted as a function of F using parameters from Table 1 and Eq. (14). Continuous line: $h = 0$ mm, dash-dot line: $h = 10$ mm, dash-dot-dot line: $h = 15$ mm. Data are from Auger electron measurements with $h = 15$ mm [14].

tron spectroscopy data taken with our spectrometer [15], the basic parameters of which are listed in Table 1, are also shown in Fig. 3. These measurements are seen to be smaller than theory for the same h ($h = 15$ mm), possibly indicating that the performance of our actual (including fringing fields) lens + HDA is better than predicted. Further investigations, possibly including fringing field effects in an electron-optics simulation program will be pursued to gain more understanding of these results.

3. Summary and conclusions

In conclusion, we have presented a very simple method for obtaining the ultimate base resolution of a hemispherical deflector analyzer as well as the linear magnification of the associated lens system under the constraints of the Helmholtz–Lagrange law for conjugate object–image pairs. The analytic results obtained can be readily used in the design and performance evaluation of such a spectrometer. Our method can in principle be extended with some modifications to include all particle spectrometers utilizing a virtual entry slit the size of which is controlled by a lens, and should therefore be of general interest to the spectroscopy community at large.

Acknowledgement

We would like to thank Prof. George C. King for useful communications. This work was partially supported by the Division of Chemical Sciences, Geosciences and Biosciences, Office of Basic Energy Sciences, Office of Science, US Department of Energy.

References

[1] B. Wannberg, A. Sköllermo, J. Electr. Spectr. Rel. Phenom. 10 (1977) 45.
[2] J.E. Pollarhid, D.J. Trevor, Y.T. Lee, D.A. Shirley, Rev. Sci. Instr. 52 (1981) 1837.
[3] P. Baltzer, B. Wannberg, M.C. Göthe, Rev. Sci. Instr. 62 (1991) 643.
[4] P.W. Lorraine, B.D. Thoms, W. Ho, Rev. Sci. Instr. 63 (1992) 1652.
[5] N. Mårtensson, P. Baltzer, P.A. Brühwiler, J.O. Forsell, A. Nilsson, A. Stenborg, B. Wannberg, J. Electr. Spectr. Rel. Phenom. 70 (1994) 117.
[6] T.J.M. Zouros, E.P. Benis, J. Electr. Spectr. Rel. Phenom. 125 (2002) 221;
T.J.M. Zouros, E.P. Benis, J. Electr. Spectr. Rel. Phenom. 142 (2005) 175–176 (corrigendum).
[7] V.P. Afanas'ev, S.Y. Yavor, Sov. Phys. Tech. Phys. 20 (1976) 715, note [Translation of Zh. Tekh. Fiz. 45, 1137-70 (1975)].
[8] E. Granneman, M.V. der Wiel, in: E.-E. Koch (Ed.), Handbook of Synchrotron Radiation, Vol. 1, North Holland Publishing Company, Amsterdam, 1983, p. 367.
[9] G.K. Ovrebo, J.L. Erskine, J. Electr. Spectr. Rel. Phenom. 24 (1981) 189.
[10] J.L. Erskine, Expt. Meth. Phys. Sci. 29A (1995) 209.
[11] G.C. King, Expt. Meth. Phys. Sci. 29A (1995) 189.
[12] T.J.M. Zouros, E.P. Benis, Appl. Phys. Lett. 86 (2005) 0941059.
[13] T.J.M. Zouros, J. Electr. Spectr. Rel. Phenom. to be published.
[14] E.P. Benis, Ph.D. dissertation, Department of Physics, University of Crete, 2001, unpublished.
[15] E.P. Benis, T.J.M. Zouros, T.W. Gorczyca, A.D. González, P. Richard, Phys. Rev. A 69 (2004) 052718.